Article

Epiregulin (EREG) is upregulated through an IL-1β autocrine loop in Caco-2 Epithelial Cells with Reduced CFTR Function[†]

Macarena Massip-Copiz, Mariángeles Clauzure, Ángel G. Valdivieso, and Tomás A. Santa-Coloma*

Running head: CFTR regulates *EREG* expression

From the Laboratory of Cellular and Molecular Biology, Institute for Biomedical Research (BIOMED), School of Medical Sciences, Pontifical Catholic University of Argentina (UCA), and the National Scientific and Technical Research Council (CONICET), Buenos Aires, Argentina.

[*]Corresponding author: Tomás A. Santa Coloma, Instituto de Investigaciones Biomédicas (BIOMED), Facultad de Ciencias Médicas, Pontificia Universidad Católica Argentina, Alicia Moreau de Justo 1600, Buenos Aires C1107AFF, Argentina. Tel/Fax: 5411-4338-0886. E-mail: tsantacoloma@gmail.com, tomas_santacoloma@uca.edu.ar

Additional Supporting Information may be found in the online version of this article.

1

Abstract

CFTR is a cAMP-regulated chloride channel, whose mutations produce cystic fibrosis. The impairment of CFTR activity increases the intracellular Cl^- concentration, which in turn produces an increased interleukin-1β (IL-1β) secretion. The secreted IL-1β then induces an autocrine positive feedback loop, further stimulating IL-1β priming and secretion. Since IL-1β can transactivate the epidermal growth factor receptor (EGFR), we study here the levels of expression for different EGFR ligands in Caco-2/pRS26 cells (expressing shRNA against CFTR resulting in a reduced CFTR expression and activity). The epiregulin (*EREG*), amphiregulin (*AREG*) and heparin binding EGF like growth factor (*HBEGF*) mRNAs, were found overexpressed in Caco-2/pRS26 cells. The *EREG* mRNA had the highest differential expression and was further characterized. In agreement with its mRNA levels, Western blots (WB) showed increased EREG levels in CFTR-impaired cells. In addition, *EREG* mRNA and protein levels were stimulated by incubation with exogenous IL-1β and inhibited by the Interleukin 1 receptor type I (IL1R1) antagonist IL1RN, suggesting that the overexpression of *EREG* is a consequence of the autocrine IL-1β loop previously described for these cells. In addition, the JNK inhibitor SP600125, and the EGFR inhibitors AG1478 and PD168393, also had an inhibitory effect on *EREG* expression, suggesting that EGFR, activated in Caco-2/pRS26 cells, is involved in the observed *EREG* upregulation. In conclusion, in Caco-2 CFTR-shRNA cells, the EGFR ligand EREG is overexpressed due to an active IL-1β autocrine loop that indirectly activates EGFR, constituting new signaling effectors for the CFTR signaling pathway, downstream of CFTR, Cl^- and IL-1β. This article is protected by copyright. All rights reserved

3

Introduction

Epiregulin (EREG) is a member of the epidermal growth factor (EGF) family. It was first purified from conditioned medium of the mouse fibroblast tumour-derived cell line NIH3T3/T7 as a 46 kDa protein [Toyoda et al., 1995]. EREG is initially expressed as an extracellular transmembrane protein, which is cleaved by disintegrins and metalloproteinases (ADAMs) enzymes to give its mature soluble form [Riese and Cullum, 2014]. Although EREG was found to be upregulated in many types of cancer, such as bladder, gastric, colorectal, breast, lung, head and neck, and liver [Riese and Cullum, 2014], it also plays an important role in inflammation [Harada et al., 2015], wound-healing [Pastore et al., 2008], and normal physiology [Riese and Cullum, 2014]. Primarily, it participates in proliferation, migration and differentiation processes [Inatomi et al., 2006; Riese and Cullum, 2014; Vermeer et al., 2006]. Interestingly, it was found that EREG contributes to the pathogenesis of rheumatoid arthritis, a disease with an important inflammatory component [Lahoti et al., 2014].

On the other hand, cystic fibrosis (CF) is a rare autosomal recessive disease [Fanen et al., 2014], caused by mutations in the cystic fibrosis transmembrane conductance regulator (*CFTR*) gene [Riordan et al., 1989; Rommens et al., 1989]. Among other symptoms, it is characterized by a persistent inflammatory condition [Nichols and Chmiel, 2015; Rottner et al., 2009] and chronic bacterial lung infections [Caverly et al., 2015], leading in the long term to a severe and lethal lung malfunction [Harun et al., 2016]. Despite the enormous effort done in the last 25 years, the exact mechanism by which the CFTR induces the complex CF phenotype is largely unknown. After the CFTR was cloned, most studies focused in the non-genomic effects of CFTR. Due to the complexity of the CF phenotype, we speculated at that

4

time that such phenotype might be the result of a complex net of genes modulated somehow by the CFTR activity. Thus, using differential display, several CFTR-dependent genes were found. Among them c-Src, responsible for the overexpression of MUC1 [Gonzalez-Guerrico et al., 2002], and the mitochondrial proteins CISD1 [Taminelli et al., 2008] and MTND4 [Valdivieso et al., 2007]. Almost simultaneously, other investigators also found CFTR-dependent genes by using microarrays [Eidelman et al., 2001; Srivastava et al., 1999; Xu et al., 2003]. Therefore, the hypothesis of the existence of CFTR-dependent genes was well-supported. On the other hand, since MTND4 was a key factor for the activity of the mitochondrial Complex I (mCx-I), and this protein was found reduced in CF cells [Valdivieso et al., 2007], we then measured the activity of this complex. As expected, its activity was found reduced in cells with impaired CFTR activity (cells with CFTR activity diminished by means of CFTR mutations, CFTR inhibitors or shRNA) [Valdivieso et al., 2012]. Noteworthy, Shapiro and colleagues also found a reduction in the mCx-I activity and other mitochondrial functions, postulating the hypothesis that the CF gene might encode a mitochondrial protein [Shapiro, 1989]. However, his mitochondrial hypothesis was disregarded when the CFTR was cloned, since it was found to be a chloride channel and not a mitochondrial protein. Nevertheless, with the reduction found later in the mCx-I activity, it became evident that Burt Shapiro was right in the sense that CF implicated in some degree a mitochondrial failure, although indirectly, through the CFTR channel, as it was previously discussed [Valdivieso and Santa-Coloma, 2013].

Now the question is how the CFTR channel induces the signals that modulate the CFTR-dependent genes. Previous results from our laboratory pointed-out c-Src as the first element in the CFTR signaling pathway, linking the reduction of the CFTR activity with MUC1 overexpression [Gonzalez-Guerrico et al., 2002]. Thus, c-Src was the first effector found for

5

the CFTR signaling pathway. In addition, IL-1β was able to regulate the expression of CFTR [Cafferata et al., 2000], modulating the activity of NF-κB [Cafferata et al., 2001]. Later, we found that an IL-1β autocrine loop was responsible for the reduction of the mCx-I activity and the overproduction of reactive oxygen species (ROS) in cells with impaired CFTR activity [Clauzure et al., 2014]. And recently, IL-1β was located upstream of c-Src in the CFTR signaling pathway [Massip-Copiz et al., 2017; Massip Copiz and Santa Coloma, 2016]. Also, the existence of several Cl⁻-dependent genes was reported [Valdivieso et al., 2016], and it was demonstrated that Cl⁻ modulates the expression of IL-1β, acting as a second messenger for CFTR [Clauzure et al., 2016]. This last result was central, since it defines the first element in the CFTR signaling pathway: the anion Cl⁻ (obvious but it was not previously demonstrated). These results also implied that Cl⁻, depending on the intracellular concentration, may act as a pro-inflammatory factor, inducing the secretion of IL-1β (maximal secretion at 75 mM Cl⁻), which in turn starts the autocrine positive feedback loop [Clauzure et al., 2016].

Now, since the IL-1β could transactivate the epidermal growth factor receptor (EGFR) in other model system [Lee et al., 2015], we hypothesized that CF cells, having increased secretion of IL-1β, might up-regulate the expression of EGFR ligands. The results obtained here, using Caco-2/pRS26 cells (cloned from Caco-2 cells stably transfected with a CFTR-shRNA), showed increased mRNA expression of the EGFR ligands epiregulin (*EREG*), amphiregulin (*AREG*) and heparin binding EGF like growth factor (*HBEGF*), having *EREG* maximal differential expression. In addition, externally added IL-1β increased *EREG* expression in Caco-2/pRSctrl cells to values comparable to those of Caco-2/pRS26 cells (cells with impaired CFTR activity). The increased *EREG* levels observed in Caco-2/pRS26 cells were significantly reduced by incubation with the interleukin 1 receptor antagonist (IL1RN), suggesting that the IL-1β autocrine loop previously described in these cells [Clauzure et al.,

6

2016; Clauzure et al., 2014; Massip-Copiz et al., 2017; Massip Copiz and Santa Coloma, 2016] was modulating the *EREG* overexpression. In addition, the EGFR was activated in Caco-2/pRS26 cells and EGFR inhibitors reduced the *EREG* overexpression, suggesting that the *EREG* overexpression is modulated by the EGFR activation (independent of ligand, since the ADAMs inhibitor TAPI-2 had no effects). The JNK inhibitor SP600125 also reduced the *EREG* upregulation. Therefore, the impairment of the CFTR activity induces IL-1β expression [Clauzure et al., 2016; Clauzure et al., 2014], which in turn indirectly stimulates EREG expression, at least partially through EGFR and JNK activation.

Materials and Methods

Reagents – Dimethyl sulfoxide (DMSO, culture grade), luminol, *p-c*oumaric acid, (2)-isoproterenol hydrochloride, protease inhibitor cocktail (Cat. No. P2714) and the interleukin 1 receptor antagonist IL1RN were purchased from Sigma-Aldrich (St. Louis, MO). Nitroblue tetrazolium (NBT) and 5-bromo-4-chloro-3-indolyl-phosphate (BCIP) were from Promega (Madison, WI), and Coomassie Brilliant Blue G-250 was from Bio-Rad Laboratories (Hercules, CA). All other reagents were analytical grade. Antibodies: goat anti-rabbit antibody coupled to alkaline phosphatase (goat polyclonal, Santa Cruz Biotechnology Cat# sc-2007 RRID:AB_631740), mouse anti p-JNK (G-7 mAb, IgG1, Santa Cruz Biotechnology Cat# sc-6254 RRID:AB_628232) and mouse anti ERK 2 (D-2 mAb, Santa Cruz Biotechnology Cat# sc-1647, RRID:AB_627547) were from Santa Cruz Biotechnology Inc. (Santa Cruz, CA), anti-rabbit antibody coupled to horseradish peroxidase (polyclonal, W401B) and anti-mouse antibody coupled to horseradish peroxidase (polyclonal, W402B) were from Promega; rabbit anti-actin antibody (polyclonal, Sigma-Aldrich Cat# A2066 RRID:AB_476693) was from

7

Sigma-Aldrich, goat anti-epiregulin antibody (polyclonal, R and D Systems Cat# AF1195 RRID:AB_354661) was from R&D Systems Inc. (Minneapolis, MN), mouse anti p-p44/42 MAPK (Erk1/2) (Thr202/Tyr204) (E10 mAb, IgG1, New England Biolabs Cat# 9106) and rabbit anti p-Akt (Thr308) (polyclonal, New England Biolabs Cat# 9275) were from New England Biolabs (Ipswich, MA), rabbit p-EGFR (Tyr1068) (polyclonal, Cell Signaling Technology Cat#2234 RRID:AB_331701) and mouse anti-Akt (pan) (40D4 mAb, IgG1, Cell Signaling Technology Cat# 2920, RRID:AB_1147620) were from Cell Signaling Technology (Danvers, MA) and mouse anti-EGFR (clone 13, mAb, IgG1, BD Biosciences Cat# 610016, RRID:AB_397435) was from BD Biosciences (San José, CA). The CFTR inhibitors AG1478 and PD168393, and the ADAMs inhibitor TAPI-2, were from MCE (MedChem Express, Monmouth Junction, NJ).

Cell Cultures – Caco-2 cells (ATCC Cat# HTB-37, RRID:CVCL_0025; human colon carcinoma epithelial cells) expressing wt-CFTR [Sood et al., 1992; Tien et al., 1994] were previously selected and cloned after transfections with short hairpin RNA interference (shRNA) directed against CFTR and a control plasmid [Valdivieso et al., 2012]. These cells were cultured adding 2 µg/ml puromycin to the culture medium for cells expansion, and without puromycin during the experiments. All cells were cultured in DMEM/F12 (Life Technologies, GIBCO BRL products, Rockville, MD) supplemented with 5% FBS (Internegocios S.A., Mercedes, Buenos Aires, Argentina), 100 units/ml penicillin, 100 µg/ml streptomycin (Life Technologies, GIBCO BRL, Rockville, MD). Cells were seeded at a density of 50.000 cells/cm^2 in p60 dishes (~ 20 cm^2, CellStar dishes, Greiner Bio-One) and cultured for 24 h in 3 ml (150 µl/cm^2) DMEM-F12 plus 5% FBS, at 37°C in a humidified air atmosphere containing 5% CO_2. Before treatments, cells were cultured 24 h in serum-free

8

medium. The different treatments (pathway signaling inhibitors, IL-1β and IL1RN) were performed in this second 24 h period, in serum-free media. The experiments were performed in the absence of serum (for a period of 24-48 h) to avoid the possible effects of serum components that might be present in excess in the fetal bovine serum compared to the human serum accessible to epithelial cells in the intact human tissue (growth factors, etc.). The relevance of these effects was pointed-out by Ye and Lotan [Ye and Lotan, 2008] and were also discussed elsewhere [Massip Copiz and Santa Coloma, 2016] .

Protein extraction – Cells were incubated as above indicated, washed twice with cold PBS, scraped with cold extraction buffer (10 mM Tris pH 7.4, 100 mM NaCl, 0.1% SDS, 0.5% sodium deoxycholate, 1% Triton X-100, 10% glycerol) containing the protease inhibitor cocktail P2714 (5 ml of cocktail/20 g of cell extract) plus phosphatase inhibitors (2 mM Na_3VO_4, 1 mM NaF and 10 mM Na_2PO_7), and centrifuged at 14000 x g for 20 min at 4° C. The supernatant was stored at -80 °C until use. The protein concentration was measured by using the method of Lowry et al. [Lowry, 1951].

Western Blots– Western blots were performed to quantify EREG, p-JNK and actin, as previously described for c-Src and p-P38 [Cafferata et al., 2001; Clauzure et al., 2014; Gonzalez-Guerrico et al., 2002]. Briefly, cytosolic extracts (30-50 μg of proteins) were separated on a denaturing SDS-PAGE (11% acrylamide/bis-acrylamide) and transferred to nitrocellulose membranes using a transfer buffer containing 20% methanol (39 mM glycine, 48 mM Tris-base, 0.037% SDS, pH 8.3) for 2 h at 100 V (constant voltage). The membranes were blocked with 5% BSA 1 h in TBST buffer (TBS pH 7 plus Tween-20 0.1% v/v) and incubated with an antibody raised against EREG (from R&D Systems, dilution 1:1000 in

9

TBST buffer) or against p-JNK (from Santa Cruz Biotechnology Inc., dilution 1:500 in TBST buffer). The membranes were then washed three times with TBST buffer, incubated with the secondary antibody and developed. Results were visualized by using an ImageQuant LAS 4000 system (GE Healthcare Life Sciences, Piscataway, NJ). Finally, as internal control, the membranes were incubated with a polyclonal anti-actin antibody (Sigma-Aldrich, A2066, dilution 1:1000 in TBST buffer) for 1 h, washed three times with TBST buffer, and then incubated with the secondary antibody and developed as above indicated. The bands intensities were quantified by using the Image J software (http://rsbweb.nih.gov).

Reverse Transcription and Quantitative Real-time PCR (qRT-PCR) - Real-time PCRs (qRT-PCR) were performed as previously described [Valdivieso et al., 2012]. qRT-PCR reactions were carried out in triplicates (intra-assay and inter-assay triplicates). The final quantification values were expressed as the mean of the Relative Quantification (RQ) for each biological triplicate (n= 3). Primer sequences used in this paper are listed in Table 1.

Statistics – Unless otherwise indicated, the assays were performed at least by duplicates (intra-assay duplicates) and the experiments were repeated three times (inter-assay triplicates), as specified in each figure legend. The results were expressed as mean $\pm$ SE (n), obtained from inter-assay calculations. One-way ANOVA and the Tukey's test were applied to calculate significant differences among samples (α= 0.05). * indicates significant differences ($p < 0.05$).

Results

Expression of EGFR ligands in Caco-2 cells transfected with shRNA specific for CFTR - First we studied the expression of different EGFR ligands in Caco-2/pRS26 cells (which are Caco-2

10

cells transfected with a plasmid that expresses a shRNA against CFTR) and compared the results with those of Caco-2/pRSctrl cells (transfected with a control plasmid). These cells were previously characterized and have a reduced CFTR expression and activity, enough to trigger oxidative stress [Clauzure et al., 2014; Massip-Copiz et al., 2017; Valdivieso et al., 2012]. Caco-2/pRSctrl and Caco-2/pRS26 cells were incubated for 24 h in serum-free DMEM/F12 and the mRNA levels of different EGFR ligands were determined by qRT-PCR. As shown in Fig. 1, Caco-2/pRS26 cells showed increased mRNA expression of amphiregulin (*AREG*) (144 ± 6.1% vs. 100 ± 4.5% (n=3)) (Fig. 1A), heparin binding EGF like growth factor (*HBEGF*) (132.2 ± 16.7% vs. 100 ± 4.5% (n=3)) (Fig. 1B) and epiregulin (*EREG*) (231.4 ± 13.7% vs. 100 ± 2.4% (n=3)) (Fig. 1C), compared to control cells. By the contrary, a significant decrease in transforming growth factor alpha (*TGFA/TGF-α*) mRNA levels were found in Caco-2/pRS26 cells compared to control cells (76.6 ± 3.1% vs. 100 ± 2.6% (n=3)) (Fig. 1D). These results are similar to the results from Oshima et al. [Oshima et al., 2012], showing high levels of *EREG* mRNA and low levels of secreted TGFA in LU-HNSCC-6 (HN-6) cells derived from a squamous cell carcinoma from the tongue. On the other hand, no significant differences in mRNA levels of epidermal growth factor (*EGF*) (Fig. 1E) or betacellulin (*BTC*) (another EGFR ligand) (Fig. 1F) were found between these cell lines; similar levels of *EGFR* and *ERBB4* were found in both cells lines (Caco-2 shRNA and control cells) (Fig. 2C and 2D). Since *EREG* showed the highest differential expression in Caco-2/pRS26 cells (Fig. 1C), we decided to further characterize its expression by using Western blots (WB). As shown in Fig. 2A (WB) and 2B (quantification), the EREG protein levels were also significantly (p<0.05) increased in Caco-2/pRS26 cells compared to control cells, in agreement with its mRNA expression levels. The phosphorylation of EGFR, AKT and ERK

11

were also increased in Caco-2/pRS26 cells (Fig. S1), suggesting the activation of the EGFR pathway in these cells with impaired CFTR activity.

Effect of IL-1β addition on EREG expression in Caco-2/pRS26 cells - To study the possible role of IL-1β in the upregulation of *EREG*, we first tested whether the addition of exogenous IL-1β could increase *EREG* levels in Caco-2/pRSctrl and Caco-2/pRS26 cells. Both cell lines were incubated with 5 ng/ml of IL-1β for 24 h in serum-free medium. As shown in Figure 3A, *EREG* expression in Caco-2/pRSctrl cells was significantly increased ($p<0.05$) by IL-1β compared to untreated control cells (Caco-2/pRSctrl $100 \pm 2.5\%$ vs. Caco-2/pRSctrl + IL-1β $180.9 \pm 24.5\%$, (n=3)). On the other hand, in Caco-2/pRS26 cells, the IL-1β stimulating effects over *EREG* were less pronounced (due to the already high values of untreated cells) and did not reach significance (Caco-2/pRS26 $191.9 \pm 10.3\%$ vs. Caco-2/pRS26 + IL-1β $232.7 \pm 23.5\%$, (n=3)). Interestingly, Caco-2/pRSctrl cells treated with IL-1β reached similar levels to those of Caco-2/pRS26 cells. Similar results were found when the EREG protein was measured, as shown in Figure 3B (WB) and 3C (quantification). The IL-1β effect on *EREG* expression was also observed at shorter times (1 h) (Fig. S2). Altogether, these results demonstrate that addition of exogenous IL-1β to Caco-2/pRSctrl cells results in increased EREG (mRNA and protein) expression. These observations agree with previous reports showing that IL-1β increased *EREG* mRNA expression in myofibroblasts [Inatomi et al., 2006]. The minimal response to exogenous IL-1β (5 ng/ml) observed for Caco-2/pRS26 cells suggest that these cells, with already elevated IL-1β basal levels due to its active autocrine loop [Clauzure et al., 2014], have almost a saturated response of EREG to IL-1β.

12

The IL-1β receptor antagonist IL1RN reduces the EREG expression in Caco-2/pRS26 cells - A reduction in the CFTR channel activity determines the accumulation of intracellular Cl^- in Caco-2/pRS26 cells, with the subsequent activation of the IL-1β autocrine loop [Clauzure et al., 2016; Clauzure et al., 2014; Massip-Copiz et al., 2017] (and other CFTR/Cl^--dependent genes [Taminelli et al., 2008; Valdivieso et al., 2012; Valdivieso et al., 2016; Valdivieso et al., 2007]). Thefore, we hypothesized that secreted IL-1β could be involved in the increased expression of *EREG* observed in the Caco-2/pRS26 cell line. To test this, Caco-2/pRS26 cells and Caco-2/pRSctrl control cells were incubated 24 h in serum free media with IL1RN to block the IL-1β binding to its receptor [Arend, 1990; Carter et al., 1990; Hayashi and Onozaki, 2005]. As shown in Figure 4A, incubation of Caco-2/pRS26 cells with IL1RN, decreased *EREG* mRNA expression (Caco-2/pRS26 191.9 ± 10.3% vs. Caco-2/pRS26 plus IL1RN 138.8 ± 11.1% (n=3), p<0.05). Similar results were found when the EREG protein levels were measured, as shown in Figure 4B (WB) and 4C (quantification). It should be noted here that we know from previous results that these Caco-2 cell lines express similar levels of IL1R1 [Massip-Copiz et al., 2017], so the differences should be attributed mainly to the increased IL-1β levels secreted by the Caco-2/pRS26 cells, with the impaired CFTR activity. Taken together, these results suggest that the IL-1β autocrine loop is responsible for the increased *EREG* levels observed in the Caco-2/pRS26 CFTR-impaired cells.

JNK is involved in the EREG expression stimulated by autocrine IL-1β- As a first approach to study the signaling pathways that could be involved in the increased *EREG* expression in Caco-2/pRS26 cells, the cells we incubated for 24 h in serum-free medium in the presence of different IL-1β pathway inhibitors (10 μM PP2 for c-Src [Lin et al., 2015], ED_{50} ~1 μM [Massip-Copiz et al., 2017]; 10 μM SB203580 for p38 [Xiao et al., 2017], ED_{50} 0.3-0.5 μM

13

[Lali et al., 2000]; 10 μM SP600125 for JNK [Sadok et al., 2008], ED_{50} 5-12 μM [Bennett et al., 2001]). As shown in Figure 5A, the JNK inhibitor SP600125 decreased the *EREG* mRNA expression compared to Caco-2/pRS26 untreated cells (180.1 ± 10,2% vs. 98.9 ± 17.2%, (n=3), respectively), while the c-Src inhibitor (PP2) had little effect, which did not reach significance. The p38 inhibitor (SB 203580) did not show significant differences. It is important to mention that *EREG* expression was partially inhibited by using the EGFR inhibitor AG1478 at 10 μM, and strongly inhibited by 10 μM PD168393, as shown in Fig. S3, suggesting that the EGFR activation is responsible of the elevated EREG levels in Caco-2/pRS26. On the other hand, the ADAMs activity inhibitor TAPI-2 at 20 μM [Forsyth et al., 2010], was not able to modify *EREG* expression, as shown in Fig. S4, suggesting that the EGFR activation might be, in this case, independent of ligand, as occurs for example with the GPCR/EGFR cross-talk in Leydig cells [Evaul and Hammes, 2008]. On the other hand, the inhibitory effect on *EREG* expression was particularly important with the JNK signaling pathway inhibitor SP600125, which fully restored the *EREG* mRNA levels to those of control cells (Caco-2/pRSctrl 100 ± 1.4%, Caco-2/pRS26 180.1 ± 10.2%, Caco-2/pRS26 plus SP600125 98.9 ± 17.2% and Caco-2/pRSctrl plus SP600125 66.1 ± 7.1%, (n=3)) (Figure 5B). A dose response curve for the effects of SP600125 on *EREG* expression in both cell lines are shown in Fig. S5 (ED_{50}= 2.9 ± 0.6 μM for Caco-2 control cells and 3.2 ± 0.7 μM for Caco-2/pRS26). Similar effects were observed when the EREG protein levels were measured by WBs, as shown in Figure 5C (WB) and 5D (quantification). As shown in Figure 5E (WB) and 5F (quantification), SP600125 inhibits JNK in accordance to the EREG reduction. Contrary to IL1RN, SP600125 also inhibited EREG basal values, suggesting that some other effector/pathway besides IL-1β might be also involved in *EREG* expression. These results agree with a previous report of Auf et al. showing the role of JNK pathway in *EREG*

14

expression in glioma cells [Auf et al., 2013]. Altogether, these results suggest that the JNK pathway is involved in the increased *EREG* expression observed in the CFTR-impaired Caco-2/pRS26 cells.

Discussion

Using Caco-2 cells stably transfected with a CFTR shRNA, we found here increased mRNA expression of *EREG*, *AREG*, and *HBEGF* genes. The most highly expressed gene was *EREG*, followed by *AREG* and *HBEGF*. On the other hand, *EGF*, *BTC* and *TGFA* showed a slight tendency to a reduced expression, which was only statistically significant for *TGFA*. In agreement with these results, the upregulation of *EREG* has been previously observed by other authors in human native nasal epithelial cells (collected from bilateral nasal mucosal brushing) from ΔF508-CFTR homozygotes patients in comparison to non-CF controls patients [Clarke et al., 2013].

Then, considering that Caco-2/pRS26 cells overexpress IL-1β [Clauzure et al., 2014], we explored whether the IL-1β secreted by Caco-2/pRS26 cells was responsible for the increased *EREG* expression. For this purpose, Caco-2/pRS26 cells were incubated 24 hours in serum-free media, first in the presence of exogenous (added) IL-1β, which resulted in stimulated *EREG* expression, an effect more evident in Caco-2/pRSctrl cells compared to Caco-2/pRS26 cells, demonstrating a role of IL-1β signaling modulation of the *EREG* expression. In agreement with these results, Inatomi and colleagues observed in human colonic epithelial myofibroblasts the increased *EREG* gene expression induced by exogenous IL-1β [Inatomi et al., 2006].

The response to exogenous IL-1β was less evident in Caco-2/pRS26 cells and this was likely due to the presence of a more active IL-1β loop in these cells. To test this idea, Caco-

15

2/pRS26 cells were then incubated in the presence of the IL1R1 antagonist IL1RN. In these conditions, a significant reduction in *EREG* levels (mRNA and protein) was observed in Caco-2/pRS26 cells. Thus, the autocrine IL-1β loop already described for these cells [Clauzure et al., 2016; Clauzure et al., 2014; Massip-Copiz et al., 2017] appears to be responsible, at least partially, for the increased *EREG* expression observed in Caco-2/pRS26 cells. This IL-1β autocrine loop also regulates the mitochondrial Complex-I activity, the cellular and mitochondrial ROS generation and the c-Src expression and activity in these epithelial cells [Clauzure et al., 2014; Massip-Copiz et al., 2017]. In agreement with these results, Iannitti et al. [Iannitti et al., 2016], either using a CF murine model, human bronchial epithelial cells (from ΔF508-CFTR homozygotes patients), or epidemiology analysis, have also noted the relevance of IL-1β signalling and its reversion by anakinra (IL1RN) in modulating NLRP3 inflammasome activity, which is responsible for IL-1β maturation and secretion.

Exploring the effect of different inhibitors of IL-1β signalling pathways (p38, c-Src and JNK inhibitors), we observed that JNK was involved in the *EREG* regulation, while the c-Src inhibitor PP2 had a minor effect; the p38 inhibitor had no effects. The effect of the JNK inhibitor SP600125 in *EREG* expression was observed in both Caco-2/pRS26 and Caco-2/pRSctrl. Altogether, these results suggest that JNK is involved in the signalling mechanism that stimulates *EREG* expression. Interestingly, the JNK inhibitor was able to decrease *EREG* levels to near basal values, suggesting these results that the JNK signaling is probably the main signaling pathway regulating *EREG* expression in these cells. Since the JNK inhibitor also inhibited basal values of Caco-2/pRSctrl cells and this did not occur with IL1RN, probably another effector under JNK regulation might be also involved in EREG regulation,

16

besides IL-1β. A graphical summary of the results obtained here is shown in Figure 6 (Pathway Studio v.10, Elsevier).

Diverse pathophysiological consequences might arise due to persistent high levels of EREG in CF cells and other cells with decreased CFTR activity. EREG is not only upregulated in many types of cancer [Riese and Cullum, 2014]; it also plays an important role in inflammation [Harada et al., 2015], wound-healing [Pastore et al., 2008] and normal physiology [Riese and Cullum, 2014]. However, a direct link between these functions and EREG has not been yet explored for CF cells. Further studies are needed to understand the mechanisms involved in its regulation and the possible physiopathological significance of the EREG overexpression.

17

References

Arend WP. 1990. Interleukin-1 receptor antagonist: discovery, structure and properties. Prog Growth Factor Res 2:193-205.

Auf G, Jabouille A, Delugin M, Guerit S, Pineau R, North S, Platonova N, Maitre M, Favereaux A, Vajkoczy P, Seno M, Bikfalvi A, Minchenko D, Minchenko O, Moenner M. 2013. High epiregulin expression in human U87 glioma cells relies on IRE1alpha and promotes autocrine growth through EGF receptor. BMC Cancer 13:597.

Bennett BL, Sasaki DT, Murray BW, O'Leary EC, Sakata ST, Xu W, Leisten JC, Motiwala A, Pierce S, Satoh Y, Bhagwat SS, Manning AM, Anderson DW. 2001. SP600125, an anthrapyrazolone inhibitor of Jun N-terminal kinase. Proc Natl Acad Sci U S A 98:13681-6.

Cafferata EG, Gonzalez-Guerrico AM, Giordano L, Pivetta OH, Santa-Coloma TA. 2000. Interleukin-1beta regulates CFTR expression in human intestinal T84 cells. Biochim Biophys Acta 1500:241-8.

Cafferata EG, Guerrico AM, Pivetta OH, Santa-Coloma TA. 2001. NF-kappaB activation is involved in regulation of cystic fibrosis transmembrane conductance regulator (CFTR) by interleukin-1beta. J Biol Chem 276:15441-4.

Carter DB, Deibel MR, Jr., Dunn CJ, Tomich CS, Laborde AL, Slightom JL, Berger AE, Bienkowski MJ, Sun FF, McEwan RN, et al. 1990. Purification, cloning, expression and biological characterization of an interleukin-1 receptor antagonist protein. Nature 344:633-8.

Caverly LJ, Zhao J, LiPuma JJ. 2015. Cystic fibrosis lung microbiome: opportunities to reconsider management of airway infection. Pediatr Pulmonol 50 Suppl 40:S31-8.

Clarke LA, Sousa L, Barreto C, Amaral MD. 2013. Changes in transcriptome of native nasal epithelium expressing F508del-CFTR and intersecting data from comparable studies. Respir Res 14:38.

Clauzure M, Valdivieso AG, Massip-Copiz MM, Mori C, Dugour AV, Figueroa JM, Santa-Coloma TA. 2016. Intracellular Chloride Concentration Changes Modulate IL-1beta Expression and Secretion in Human Bronchial Epithelial Cultured Cells. J Cell Biochem.

Clauzure M, Valdivieso AG, Massip Copiz MM, Schulman G, Teiber ML, Santa-Coloma TA. 2014. Disruption of interleukin-1beta autocrine signaling rescues complex I activity and improves ROS levels in immortalized epithelial cells with impaired cystic fibrosis transmembrane conductance regulator (CFTR) function. PLoS One 9:e99257.

Eidelman O, Srivastava M, Zhang J, Leighton X, Murtie J, Jozwik C, Jacobson K, Weinstein DL, Metcalf EL, Pollard HB. 2001. Control of the proinflammatory state in cystic fibrosis lung epithelial cells by genes from the TNF-alphaR/NFkappaB pathway. Mol Med 7:523-34.

Evaul K, Hammes SR. 2008. Cross-talk between G protein-coupled and epidermal growth factor receptors regulates gonadotropin-mediated steroidogenesis in Leydig cells. J Biol Chem 283:27525-33.

Fanen P, Wohlhuter-Haddad A, Hinzpeter A. 2014. Genetics of cystic fibrosis: CFTR mutation classifications toward genotype-based CF therapies. Int J Biochem Cell Biol 52:94-102.

Forsyth CB, Tang Y, Shaikh M, Zhang L, Keshavarzian A. 2010. Alcohol stimulates activation of Snail, epidermal growth factor receptor signaling, and biomarkers of epithelial-mesenchymal transition in colon and breast cancer cells. Alcohol Clin Exp Res 34:19-31.

Gonzalez-Guerrico AM, Cafferata EG, Radrizzani M, Marcucci F, Gruenert D, Pivetta OH, Favaloro RR, Laguens R, Perrone SV, Gallo GC, Santa-Coloma TA. 2002. Tyrosine kinase c-Src constitutes a bridge between cystic fibrosis transmembrane regulator channel failure and MUC1 overexpression in cystic fibrosis. J Biol Chem 277:17239-47.

Harada M, Kamimura D, Arima Y, Kohsaka H, Nakatsuji Y, Nishida M, Atsumi T, Meng J, Bando H, Singh R, Sabharwal L, Jiang JJ, Kumai N, Miyasaka N, Sakoda S, Yamauchi-Takihara K, Ogura H, Hirano T, Murakami M. 2015. Temporal expression of growth factors triggered by epiregulin regulates inflammation development. J Immunol 194:1039-46.

Harun SN, Wainwright C, Klein K, Hennig S. 2016. A systematic review of studies examining the rate of lung function decline in patients with cystic fibrosis. Paediatr Respir Rev 20:55-66.

Hayashi H, Onozaki K. 2005. [Interleukin-1 (IL-1) alpha, beta, IL-1 receptor, IL-1 receptor antagonist (IL-1ra)]. Nihon Rinsho 63 Suppl 8:60-4.

Iannitti RG, Napolioni V, Oikonomou V, De Luca A, Galosi C, Pariano M, Massi-Benedetti C, Borghi M, Puccetti M, Lucidi V, Colombo C, Fiscarelli E, Lass-Florl C, Majo F, Cariani L, Russo M, Porcaro L, Ricciotti G, Ellemunter H, Ratclif L, De Benedictis FM, Talesa VN, Dinarello CA, van de Veerdonk FL, Romani L. 2016. IL-1 receptor antagonist ameliorates inflammasome-dependent inflammation in murine and human cystic fibrosis. Nat Commun 7:10791.

Inatomi O, Andoh A, Yagi Y, Bamba S, Tsujikawa T, Fujiyama Y. 2006. Regulation of amphiregulin and epiregulin expression in human colonic subepithelial myofibroblasts. Int J Mol Med 18:497-503.

Lahoti TS, Hughes JM, Kusnadi A, John K, Zhu B, Murray IA, Gowda K, Peters JM, Amin SG, Perdew GH. 2014. Aryl hydrocarbon receptor antagonism attenuates growth factor expression, proliferation, and migration in fibroblast-like synoviocytes from patients with rheumatoid arthritis. J Pharmacol Exp Ther 348:236-45.

Lali FV, Hunt AE, Turner SJ, Foxwell BM. 2000. The pyridinyl imidazole inhibitor SB203580 blocks phosphoinositide-dependent protein kinase activity, protein kinase B phosphorylation, and retinoblastoma hyperphosphorylation in interleukin-2-stimulated T cells independently of p38 mitogen-activated protein kinase. J Biol Chem 275:7395-402.

Lee CH, Syu SH, Liu KJ, Chu PY, Yang WC, Lin P, Shieh WY. 2015. Interleukin-1 beta transactivates epidermal growth factor receptor via the CXCL1-CXCR2 axis in oral cancer. Oncotarget 6:38866-80.

Lin TY, Fan CW, Maa MC, Leu TH. 2015. Lipopolysaccharide-promoted proliferation of Caco-2 cells is mediated by c-Src induction and ERK activation. Biomedicine (Taipei) 5:5.

Lowry OH, Rosebroug, N.J., Farr, A.L. and Randall, R.J. 1951. Protein measurement with the Folin phenol reagent. J.Biol.Chem 193:265- 275.

Massip-Copiz MM, Clauzure M, Valdivieso AG, Santa-Coloma TA. 2017. CFTR impairment upregulates c-Src activity through IL-1beta autocrine signaling. Arch Biochem Biophys 616:1-12.

Massip Copiz MM, Santa Coloma TA. 2016. c- Src and its role in cystic fibrosis. Eur J Cell Biol 95:401-413.

19

Nichols DP, Chmiel JF. 2015. Inflammation and its genesis in cystic fibrosis. Pediatr Pulmonol 50 Suppl 40:S39-56.

Oshima G, Wennerberg J, Yamatodani T, Kjellen E, Mineta H, Johnsson A, Ekblad L. 2012. Autocrine epidermal growth factor receptor ligand production and cetuximab response in head and neck squamous cell carcinoma cell lines. J Cancer Res Clin Oncol 138:491-9.

Pastore S, Mascia F, Mariani V, Girolomoni G. 2008. The epidermal growth factor receptor system in skin repair and inflammation. J Invest Dermatol 128:1365-74.

Riese DJ, 2nd, Cullum RL. 2014. Epiregulin: roles in normal physiology and cancer. Semin Cell Dev Biol 28:49-56.

Riordan JR, Rommens JM, Kerem B, Alon N, Rozmahel R, Grzelczak Z, Zielenski J, Lok S, Plavsic N, Chou JL, et al. 1989. Identification of the cystic fibrosis gene: cloning and characterization of complementary DNA. Science 245:1066-73.

Rommens JM, Iannuzzi MC, Kerem B, Drumm ML, Melmer G, Dean M, Rozmahel R, Cole JL, Kennedy D, Hidaka N, et al. 1989. Identification of the cystic fibrosis gene: chromosome walking and jumping. Science 245:1059-65.

Rottner M, Freyssinet JM, Martinez MC. 2009. Mechanisms of the noxious inflammatory cycle in cystic fibrosis. Respir Res 10:23.

Sadok A, Bourgarel-Rey V, Gattacceca F, Penel C, Lehmann M, Kovacic H. 2008. Nox1-dependent superoxide production controls colon adenocarcinoma cell migration. Biochim Biophys Acta 1783:23-33.

Shapiro BL. 1989. Evidence for a mitochondrial lesion in cystic fibrosis. Life Sci 44:1327-34.

Sood R, Bear C, Auerbach W, Reyes E, Jensen T, Kartner N, Riordan JR, Buchwald M. 1992. Regulation of CFTR expression and function during differentiation of intestinal epithelial cells. EMBO J 11:2487-94.

Srivastava M, Eidelman O, Pollard HB. 1999. Pharmacogenomics of the cystic fibrosis transmembrane conductance regulator (CFTR) and the cystic fibrosis drug CPX using genome microarray analysis. Mol Med 5:753-67.

Taminelli GL, Sotomayor V, Valdivieso AG, Teiber ML, Marin MC, Santa-Coloma TA. 2008. CISD1 codifies a mitochondrial protein upregulated by the CFTR channel. Biochem Biophys Res Commun 365:856-62.

Tien XY, Brasitus TA, Kaetzel MA, Dedman JR, Nelson DJ. 1994. Activation of the cystic fibrosis transmembrane conductance regulator by cGMP in the human colonic cancer cell line, Caco-2. J Biol Chem 269:51-4.

Toyoda H, Komurasaki T, Uchida D, Takayama Y, Isobe T, Okuyama T, Hanada K. 1995. Epiregulin. A novel epidermal growth factor with mitogenic activity for rat primary hepatocytes. J Biol Chem 270:7495-500.

Valdivieso AG, Clauzure M, Marin MC, Taminelli GL, Massip Copiz MM, Sanchez F, Schulman G, Teiber ML, Santa-Coloma TA. 2012. The mitochondrial complex I activity is reduced in cells with impaired cystic fibrosis transmembrane conductance regulator (CFTR) function. PLoS One 7:e48059.

Valdivieso AG, Clauzure M, Massip-Copiz M, Santa-Coloma TA. 2016. The Chloride Anion Acts as a Second Messenger in Mammalian Cells - Modifying the Expression of Specific Genes. Cell Physiol Biochem 38:49-64.

Valdivieso AG, Marcucci F, Taminelli G, Guerrico AG, Alvarez S, Teiber ML, Dankert MA, Santa-Coloma TA. 2007. The expression of the mitochondrial gene MT-ND4 is downregulated in cystic fibrosis. Biochem Biophys Res Commun 356:805-9.

20

Valdivieso AG, Santa-Coloma TA. 2013. CFTR activity and mitochondrial function. Redox Biol 1:190-202.

Vermeer PD, Panko L, Karp P, Lee JH, Zabner J. 2006. Differentiation of human airway epithelia is dependent on erbB2. Am J Physiol Lung Cell Mol Physiol 291:L175-80.

Xiao YT, Yan WH, Cao Y, Yan JK, Cai W. 2017. P38 MAPK Pharmacological Inhibitor SB203580 Alleviates Total Parenteral Nutrition-Induced Loss of Intestinal Barrier Function but Promotes Hepatocyte Lipoapoptosis. Cell Physiol Biochem 41:623-634.

Xu Y, Clark JC, Aronow BJ, Dey CR, Liu C, Wooldridge JL, Whitsett JA. 2003. Transcriptional adaptation to cystic fibrosis transmembrane conductance regulator deficiency. J Biol Chem 278:7674-82.

Ye X, Lotan R. 2008. Potential misinterpretation of data on differential gene expression in normal and malignant cells in vitro. Brief Funct Genomic Proteomic 7:322-6.

Figure Legends

Fig. 1. EGFR ligands expression in Caco-2/pRS26 cells. Caco-2/pRSctrl and Caco-2/pRS26 were incubated 24 h in 5% FBS and 24 h in serum-free medium. After incubation, total RNA was extracted and the mRNA levels of each ligand were measure by real-time PCR. A: Quantitative real time RT-PCR of *AREG* mRNA expression levels in Caco-2/pRSctrl and Caco-2/pRS26 cells. B: Quantitative real time RT-PCR of *HBEGF* mRNA expression levels in Caco-2/pRSctrl and Caco-2/pRS26 cells. C: Quantitative real time RT-PCR of *EREG* mRNA expression levels in Caco-2/pRSctrl and Caco-2/pRS26 cells. D: Quantitative real time RT-PCR of *TGFA* mRNA expression levels in Caco-2/pRSctrl and Caco-2/pRS26 cells. E: Quantitative real time RT-PCR of *EGF* mRNA expression levels in Caco-2/pRSctrl and Caco-2/pRS26 cells. F: Quantitative real time RT-PCR of *BTC* mRNA expression levels in Caco-2/pRSctrl and Caco-2/pRS26 cells. The results were expressed as percentage (%) relative to Caco-2/pRSctrl values (mean ± SE, n=3, inter-assay values of three independent experiments). * indicates p<0.05.

Fig. 2. EREG expression in Caco-2/pRS26 cells. Caco-2/pRSctrl and Caco-2/pRS26 were incubated 24 h in 5% FBS and 24 h in serum-free medium. After incubation, total proteins or total RNA were extracted and the *EREG* levels and *EGFRs* mRNA were determined by WBs or real-time PCR. A: Representative WB corresponding to EREG from whole cellular lysates of Caco-2/pRSctrl and Caco-2/pRS26 cells. B: Densitometric quantification of EREG/actin. C: Quantitative real time RT-PCR of *EGFR* mRNA expression levels in Caco-2/pRSctrl and Caco-2/pRS26 cells. D: Quantitative real time RT-PCR of *ERBB4* mRNA expression levels in

22

Caco-2/pRSctrl and Caco-2/pRS26 cells. The results were expressed as percentage (%) relative to Caco-2/pRSctrl values (mean ± SE, n=3, inter-assay values of three independent experiments). * indicates p<0.05.

Fig. 3. EREG expression in Caco-2/pRS26 treated with IL-1β. Caco-2/pRSctrl and Caco-2/pRS26 cells were cultured 24 h in 5% FBS and 24 h in serum-free medium before treatments for another 24 h. Cells were incubated with 5 ng/ml IL-1β. After incubation, total RNA or total proteins were extracted and the *EREG* mRNA or protein levels were determined by real-time PCR or WBs. A: Quantitative real time RT-PCR of *EREG* mRNA expression levels in Caco-2/pRSctrl and Caco-2/pRS26 cells treated with IL-1β. B: Representative WB corresponding to EREG from whole cellular lysates of Caco-2/pRSctrl and Caco-2/pRS26 cells. C: Densitometric quantification of EREG/actin. The results were expressed as percentage (%) relative to Caco-2/pRSctrl values (mean ± SE, n=3, inter-assay). * indicates p<0.05 compared to Caco-2/pRSctrl cells or Caco-2/pRS26 untreated cells.

Fig. 4. EREG expression in Caco-2/pRS26 cells treated with IL1RN. Caco-2/pRSctrl and Caco-2/pRS26 cells were cultured 24 h in 5% FBS and 24 h in serum-free medium before treatments for another 24 h. Cells were incubated with 50 ng/ml of IL1RN. After incubation, total RNA or total proteins were extracted and the *EREG* mRNA or protein levels were determined by real-time PCR or WBs. A: Quantitative real time RT-PCR of *EREG* mRNA expression levels in Caco-2/pRSctrl and Caco-2/pRS26 cells treated with IL1RN. B: Representative WB corresponding to EREG from whole cellular lysates of Caco-2/pRSctrl and Caco-2/pRS26 cells. C: Densitometric quantification of EREG/actin. The results were

23

expressed as percentage (%) relative to Caco-2/pRSctrl values (mean ± SE, n=3, inter-assay). * indicates p<0.05 compared to Caco-2/pRSctrl cells or Caco-2/pRS26 untreated cells.

Fig. 5. EREG expression in Caco-2 cells transfected with shRNA for CFTR and treated with JNK inhibitor. Caco-2/pRSctrl and Caco-2/pRS26 cells were cultured 24 h in 5% FBS and 24 h in serum-free medium before treatments for another 24 h. Cells were incubated with 10 μM SP600125 (JNK inhibitor), 10 μM PP2 (c-Src inhibitor), and 10 μM SB203580 (p38 inhibitor). After incubation, total RNA or total proteins were extracted and the *EREG* mRNA or protein levels were determined by real-time PCR or WBs. A: Quantitative real time RT-PCR of *EREG* mRNA expression levels in Caco-2/pRSctrl and Caco-2/pRS26 cells treated with different IL-1β pathway inhibitors. B: Quantitative real time RT-PCR of *EREG* mRNA expression levels in Caco-2/pRSctrl and Caco-2/pRS26 cells treated with JNK inhibitor (SP600125). C: Representative WB corresponding to EREG from whole cellular lysates of Caco-2/pRSctrl and Caco-2/pRS26 cells. D: Densitometric quantification of EREG/actin. E: Representative WB corresponding to p-JNK from whole cellular lysates of Caco-2/pRSctrl and Caco-2/pRS26 cells. F: Densitometric quantification of p-JNK/actin. The results were expressed as percentage (%) relative to Caco-2/pRSctrl values (mean ± SE, n=3, inter-assay). * indicates p<0.05 compared to Caco-2/pRSctrl cells or Caco-2/pRS26 untreated cells.

Fig. 6: Graphic summary of the results obtained. Due to the down-modulation of the CFTR activity in Caco-2/pRS26, Cl⁻ accumulates and stimulates IL-1β/IL1B secretion, in turn inducing an autocrine positive feed-back loop [Clauzure et al., 2016; Clauzure et al., 2014; Massip-Copiz et al., 2017; Massip Copiz and Santa Coloma, 2016; Valdivieso et al., 2016]. This IL-1β autocrine loop determines increased *EREG* expression mediated through JNK.

24

Thus, EREG constitutes a new step forward in the CFTR signaling pathway, downstream of IL-1β (--| red, inhibition; → blue, stimulation; dotted arrows, previous results).

Supplementary Figure Legends:

Fig. S1. p-EGFR, p-Akt and p-Erk expression in Caco-2/pRSctrl and Caco-2/pRS26. Cells were cultured 24 h in 5% FBS and 24 h in serum-free medium. After incubation, total proteins were extracted and p-EGFR, EGFR, p-Akt, Akt, p-Erk and Erk protein levels were determined by WBs. A: Representative WB corresponding to p-EGFR and EGFR from whole cellular lysates of Caco-2/pRSctrl and Caco-2/pRS26 cells. B: Densitometric quantification of p-EGFR/EGFR. C: Representative WB corresponding to p-Akt and Akt from whole cellular lysates of Caco-2/pRSctrl and Caco-2/pRS26 cells. D: Densitometric quantification of p-Akt/Akt. E: Representative WB corresponding to p-Erk and Erk from whole cellular lysates of Caco-2/pRSctrl and Caco-2/pRS26 cells. F: Densitometric quantification of p-Erk/Erk. The results were expressed as percentage (%) relative to Caco-2/pRSctrl values (mean ± SE, n=3, inter-assay). * indicates $p<0.05$ compared to Caco-2/pRSctrl cells.

Fig. S2. EREG expression and p-EGFR levels in Caco-2/pRSctrl and Caco-2/pRS26 treated with IL-1β. Caco-2/pRSctrl and Caco-2/pRS26 cells were cultured 24 h in 5% FBS and 24 h in serum-free medium before treatments for another hour with 5 ng/ml IL-1β. After incubation, total RNA or total proteins were extracted and the *EREG* mRNA or p-EGFR and EGFR protein levels were determined by real-time PCR or WBs. A: Quantitative real time RT-PCR of *EREG* mRNA expression levels in Caco-2/pRSctrl and Caco-2/pRS26 cells treated with IL-1β. B: Representative WB corresponding to p-EGFR and EGFR from whole cellular lysates of

25

Caco-2/pRSctrl and Caco-2/pRS26 cells. C: Densitometric quantification of p-EGFR/EGFR. The results were expressed as percentage (%) relative to Caco-2/pRSctrl values (mean ± SE, n=3, inter-assay). * indicates p<0.05 compared to Caco-2/pRSctrl cells or Caco-2/pRS26 untreated cells.

*Fig. S3. EREG expression in Caco-2 cells transfected with shRNA for CFTR (*Caco-2/pRS26 cells) *and treated with the EGFR inhibitors PD168393 and AG1478.* Caco-2/pRSctrl and Caco-2/pRS26 cells were cultured 24 h in 5% FBS and 24 h in serum-free medium before treatments for another 24 h. Cells were incubated with 10 µM PD168393 and 10 µM AG1478. After incubation, total RNA was extracted and the *EREG* mRNA levels were determined by real-time PCR. Quantitative real time RT-PCR of *EREG* mRNA expression levels in Caco-2/pRSctrl and Caco-2/pRS26 cells treated with PD168393 and AG1478. The results were expressed as percentage (%) relative to Caco-2/pRSctrl values (mean ± SE, n=3, inter-assay). * indicates p<0.05 compared to Caco-2/pRSctrl cells or Caco-2/pRS26 untreated cells.

Fig. S4. EREG expression in Caco-2 cells transfected with shRNA for CFTR and treated with the ADAMs inhibitor TAPI-2. Caco-2/pRSctrl and Caco-2/pRS26 cells were cultured 24 h in 5% FBS and 24 h in serum-free medium before treatments for another 24 h. Cells were incubated with 20 µM TAPI-2. After incubation, total RNA was extracted and the *EREG* mRNA levels were determined by real-time PCR. Quantitative real time RT-PCR of *EREG* mRNA expression levels in Caco-2/pRSctrl and Caco-2/pRS26 cells treated with ADAMs inhibitor. The results were expressed as percentage (%) relative to Caco-2/pRSctrl values. * indicates p<0.05 compared to Caco-2/pRSctrl cells.

Fig. S5. EREG expression in Caco-2 cells transfected with shRNA for CFTR and treated with the JNK inhibitor SP600125. Caco-2/pRSctrl and Caco-2/pRS26 cells were cultured 24 h in 5% FBS and 24 h in serum-free medium before treatments with SP600125 for another 24 h. Cells were incubated with different SP600125 concentrations (0, 1, 5, 10 and 20 µM). After incubation, total RNA was extracted and the *EREG* mRNA levels were determined by real-time PCR. The figure shows the quantitative real time RT-PCR of *EREG* mRNA expression levels in Caco-2/pRSctrl and Caco-2/pRS26 cells treated with JNK inhibitor (SP600125). The results were expressed as percentage (%) relative to Caco-2/pRSctrl values. * indicates p<0.05 compared to Caco-2/pRSctrl cells or Caco-2/pRS26 untreated cells.

27

Table 1. List of primer sequences used for quantitative real-time PCR analysis.

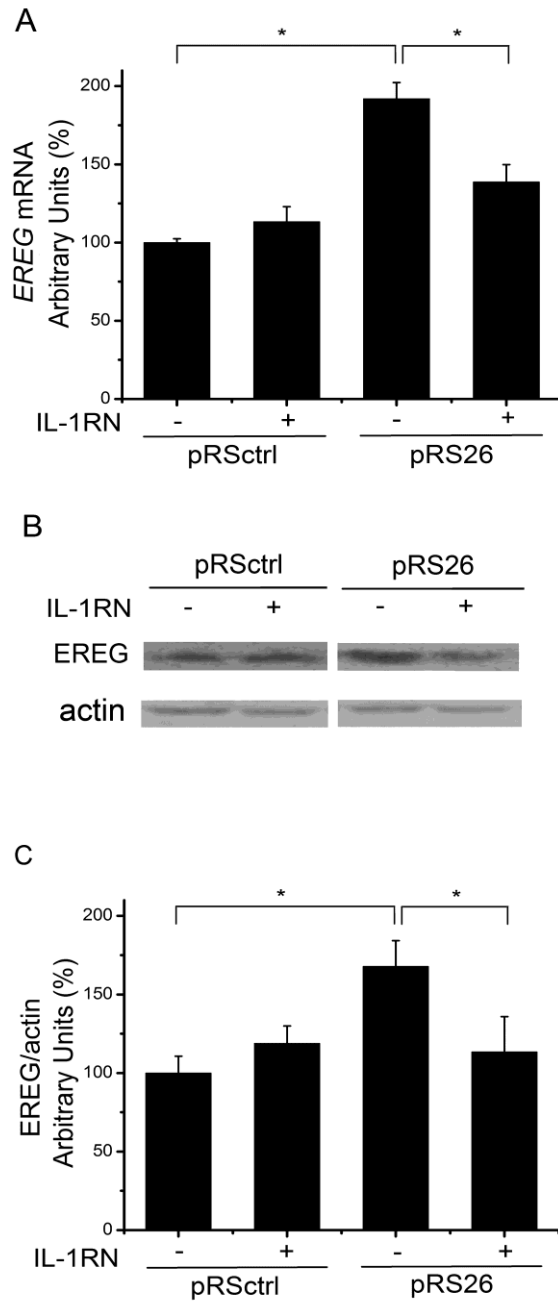| Gene		Sequence (5´- 3´)
EGFR1	Fw	GACCTCCATGCCTTTGAGAA
	Rv	GCTGACGACTGCAAGAGAAA
EGFR4	Fw	TCAAGCATTGGATAATCCCGA
	Rv	AGTGGCTCATTCACATACTCATCCT
Amphiregulin	Fw	GGTGGTGCTGTCGCTCTTG
	Rv	GGTCCCCAGAAAATGGTTCA
TGF-α	Fw	CCCTGGCTGTCCTTATCATC
	Rv	CTGTTTCTGAGTGGCAGCAA
HB-EGF	Fw	TGGAGAATGCAAATATGTGAAGGA
	Rv	AGGATGGTTGTGTGGTCATAGGTAT
EGF	Fw	TGATGGAGGTTCTGTCCACATTAGT
	Rv	CGGTCACCAAAAAGGGACAT
Epiregulin	Fw	GGACAGTGCATCTATCTGGTGGA
	Rv	AGTGTTCACATCGGACACCAGTA
Betacellulin	Fw	GGTCATCGGTGTCTGCACAT
	Rv	AGGTAACTTCATAGCCTTTTAAGCA
TBP	Fw	TGCACAGGAGCCAAGAGTGAA
	Rv	CACATC ACAGCTCCCCACCA

Figure 1

29

Figure 2

Figure 3

31

A

B

C
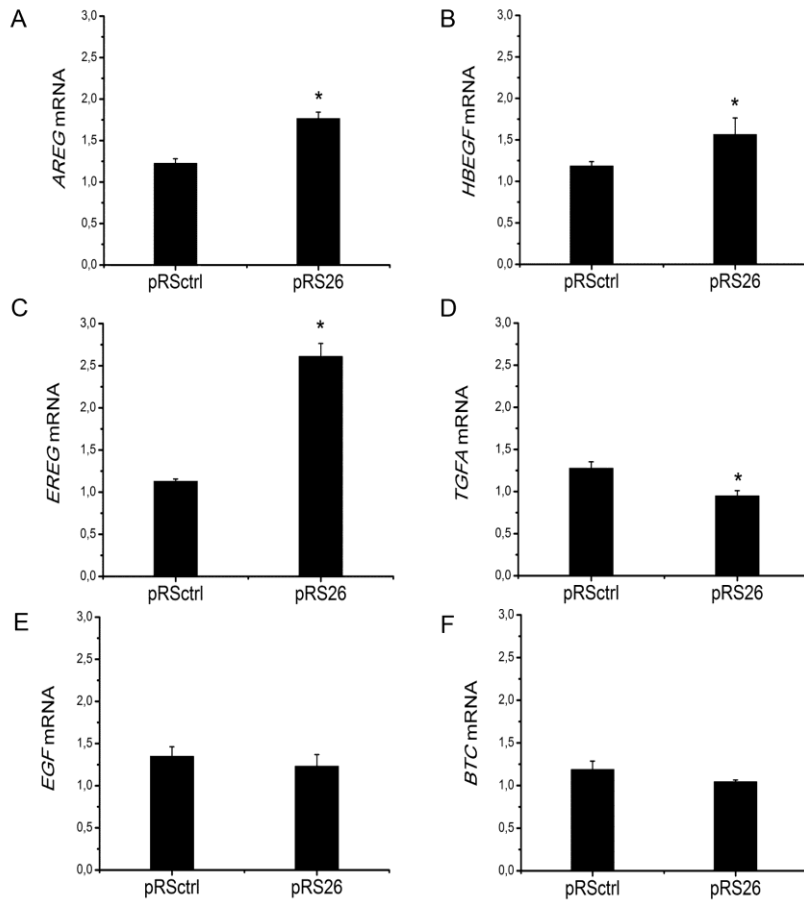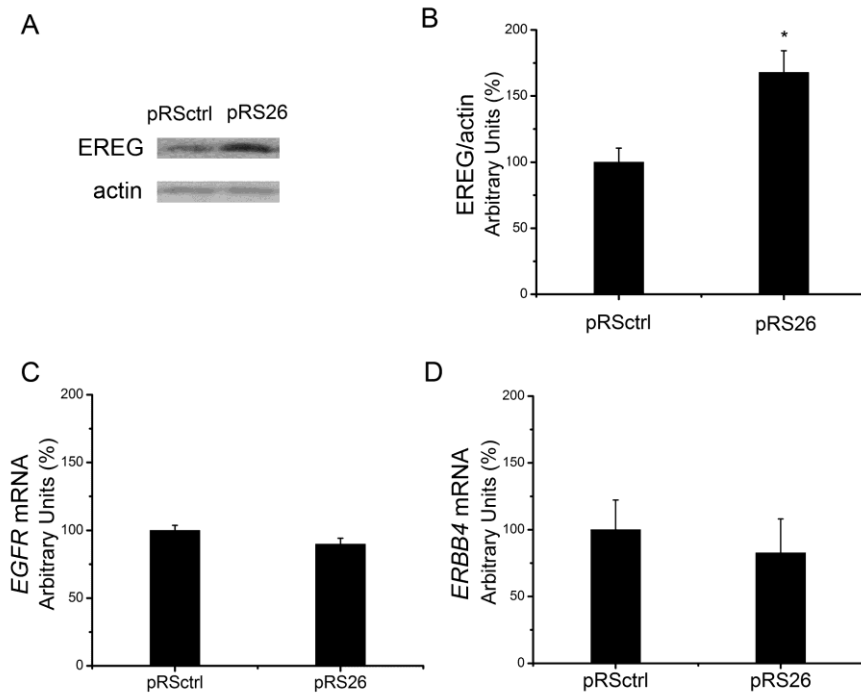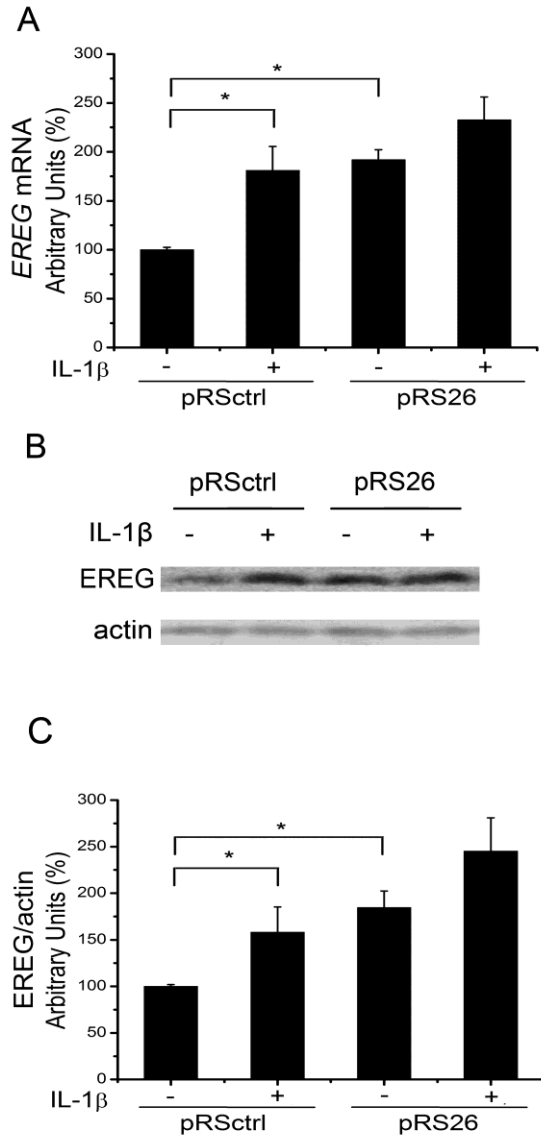
Figure 4

Figure 5

Figure 6